

Exploring Light-Cone Distribution Amplitudes from Quantum Computing

Tianyin Li,^{1,2} Xingyu Guo,^{1,2} Wai Kin Lai,^{1,2,3,*} Xiaohui Liu,^{4,5} Enke Wang,^{1,2} Hongxi Xing,^{1,2,†} Dan-Bo Zhang,^{6,7} and Shi-Liang Zhu^{6,7}

(QuNu Collaboration)

¹Guangdong Provincial Key Laboratory of Nuclear Science, Institute of Quantum Matter, South China Normal University, Guangzhou 510006, China

²Guangdong-Hong Kong Joint Laboratory of Quantum Matter,

Southern Nuclear Science Computing Center, South China Normal University, Guangzhou 510006, China

³Department of Physics and Astronomy, University of California, Los Angeles, California 90095, USA

⁴Center of Advanced Quantum Studies, Department of Physics, Beijing Normal University, Beijing 100875, China

⁵Center for High Energy Physics, Peking University, Beijing 100871, China

⁶Guangdong-Hong Kong Joint Laboratory of Quantum Matter,

Frontier Research Institute for Physics, South China Normal University, Guangzhou 510006, China

⁷Guangdong Provincial Key Laboratory of Quantum Engineering and Quantum Materials, School of Physics and Telecommunication Engineering,

South China Normal University, Guangzhou 510006, China

(Dated: October 19, 2023)

Light-cone distribution amplitudes (LCDAs) are essential nonperturbative quantities for theoretical predictions of exclusive high-energy processes in quantum chromodynamics (QCD). We demonstrate the prospect of calculating LCDAs on a quantum computer by applying a recently proposed quantum algorithm, with staggered fermions, to the simulation of the LCDA in the (1+1)-dimensional Nambu-Jona-Lasinio (NJL) model on classical hardware. The agreement between the result from the classical simulation of the quantum algorithm and that from exact diagonalization justifies the proposed quantum algorithm. We find that the resulting LCDA in the NJL model exhibits features shared with the LCDAs obtained from QCD.

PACS numbers: 03.67.Lx, 14.20.Dh, 71.10.Fd

Keywords: Light-cone distribution amplitude, Quantum algorithm, NJL model

I. INTRODUCTION

Light-cone distribution amplitudes (LCDAs) are quantities that describe the nonperturbative aspects of bound states in high-energy exclusive processes in quantum chromodynamics (QCD). They are complementary to the parton distribution functions (PDFs), which are nonperturbative quantities for inclusive QCD processes with incoming hadrons, such as deep-inelastic scattering of the proton at the Hadron-Electron Ring Accelerator (HERA) and future Electron-Ion Colliders [1–4]. In an exclusive high-energy QCD process, up to corrections suppressed by inverse powers of a large energy scale, the scattering amplitude can be factorized into the convolution of a perturbative Wilson coefficient and a nonperturbative amplitude, the LCDA [5, 6]. A seminal example is the electromagnetic form factor $F(Q^2)$ for the process $\gamma^* \gamma \rightarrow q\bar{q} \rightarrow \pi^0$ at large momentum transfer Q , for which the factorization reads

$$F(Q^2) = f_\pi \int_0^1 dx T_H(x, Q^2; \mu) \phi_\pi(x; \mu) + \mathcal{O}(\Lambda_{\text{QCD}}^2/Q^2), \quad (1)$$

where Q^2 is the 4-momentum squared carried by the virtual photon γ^* , Λ_{QCD} is the energy scale below which QCD becomes nonperturbative, and μ is the factorization scale, which separates the short-distance physics from the long-distance wave function ϕ_π . Here, $T_H(x, Q^2; \mu)$ is the hard kernel, which describes the production of a quark-antiquark pair by short-distance dynamics. $T_H(x, Q^2; \mu)$ is perturbatively calculable as an expansion in the strong coupling constant α_s . The wave function $\phi_\pi(x, \mu)$ and the factor f_π are the LCDA and the decay constant of the neutral pion, respectively. They together encode the hadronization of a quark-antiquark pair into a pion, and are nonperturbative as they are sensitive to the long-distance dynamics of QCD. The LCDA of a meson can be viewed as the probability amplitude to find the valence $q\bar{q}$ Fock state in which the quark q and the antiquark \bar{q} carry respectively the momentum fraction x and $1-x$ of the highly boosted meson. The decay constant is defined as the overall normalization of the LCDA. The LCDAs and decay constants for baryons can be likewise defined. The LCDAs, being the essential ingredients for reliable predictions for exclusive QCD processes, have been studied intensively in various directions. Early studies include their perturbative evolution with the scale μ and their asymptotic behaviors [5–7]. Estimations of the LCDAs using sum rules, illustrative models, [8–17], light-front quantization [18–21], as well as the refactorization in the nonrelativistic expansion [22, 23] have also

* wkilai@m.scnu.edu.cn

† hxing@m.scnu.edu.cn

been discussed under various circumstances in the literature. Evaluations of the LCDAs in lattice QCD were initially performed by taking the moments [24–29], and later with direct calculations in the momentum fraction x within the large momentum effective theory (LaMET) framework [30–33]. There are two major obstacles to acquiring knowledge about the LCDAs, the first being the elusiveness of the relevant experimental data that hinders QCD global analyses, the second being the nature of real-time evolution on the light cone involved in the definition of LCDAs, which is not amenable to direct evaluations using Euclidean lattice QCD [34].

Stimulated by the promising prospect of quantum computing [35], there has been a rapidly growing wave of research on applications of quantum computing in elementary particle physics [36–38]. Early theoretical attempts had showed that quantum computation costs polynomial time in simulations of real time dynamics in quantum field theory [39–42]. Validity of quantum computing in various problems in particle physics have been studied by proposals of quantum algorithms as well as simulations with real quantum computers or classical hardware. These studies include evaluations of nonperturbative quantities [43–53], simulations of real-time processes [54–62], as well as evaluations of thermodynamical quantities at finite chemical potential [63, 64].

Recently, a quantum algorithm was proposed for both the preparation of a hadron state and the evaluation of real-time light-like correlators in Ref. [51]. The algorithm was demonstrated feasible by evaluating directly the parton distribution function in the (1+1)-dimensional Nambu-Jona-Lasinio (NJL) model with staggered fermions on classical hardware. The results obtained from the quantum algorithm were checked against exact diagonalization to find full agreements, which justifies the validity of the algorithm and suggests the possibility of evaluating the hadron parton distributions in QCD by quantum computation.

In this study, we extend the previous studies to apply the quantum algorithm to study the LCDA in the (1 + 1)D 1-flavor NJL model, using staggered fermions. In Sec. II, we provide the operator definition of the LCDA in the (1+1)D NJL model. Then we present the quantum algorithm for both the hadronic state preparation and the direct computation of the quark-antiquark correlator in Sec. III. By implementing the proposed algorithm on classical hardware, we found good consistency between the results obtained from the quantum algorithm and exact diagonalization. The final results for the LCDA are presented in Sec. IV. We give a summary in Sec. V.

II. LIGHT-CONE DISTRIBUTION AMPLITUDE AND THE NJL MODEL

The LCDA of a meson h is defined as

$$\phi_h(x) = \frac{1}{f_h} \int dz e^{-i(x-1)n \cdot Pz} \times \langle \Omega | \bar{\psi}(zn) \gamma^+ W(zn, 0) \psi(0) | h(P) \rangle, \quad (2)$$

where P is the momentum of the meson and n is a light-like vector defined by $n = (1, -\hat{n})$, with \hat{n} being a spatial unit vector along the direction of motion of the meson. The plus-component of the gamma matrix γ^μ in light-cone coordinates is denoted by γ^+ , i.e. $\gamma^+ = n \cdot \gamma$. The prefactor f_h is the decay constant, defined such that $\int_0^1 dx \phi_h(x) = 1$. The matrix element in the second line in eq. (2) describes the transition amplitude from the vacuum $|\Omega\rangle$ to the hadron state $|h(P)\rangle$ via insertion of a quark-antiquark-pair operator. The $W(zn, 0)$ is the Wilson line (gauge link) on the light cone,

$$W(zn, 0) = \mathcal{P} \exp \left(ig \int_0^z dz' A_a^+(z'n) t_a \right), \quad (3)$$

where t_a are the SU(3) fundamental generators, \mathcal{P} denotes path-ordering, and $A_a^+ = n \cdot A_a$ is the plus-component of the SU(3) gauge potential. Generally, to simulate the LCDA on a quantum computer, one has to: 1. prepare the vacuum state $|\Omega\rangle$ and the hadronic state $|h(P)\rangle$ on the quantum computer; 2. simulate the Wilson line on the quantum computer; 3. evaluate the matrix element $\langle \Omega | \mathcal{O} | h \rangle$. We will elaborate on the first and third steps later in Section III. We note that the presence of the gauge field in a gauge theory will dramatically increase the demand for quantum resources. However, as noted in ref. [51], simulating the Wilson line in the second step does not introduce substantial complexity even though the Wilson line is non-local, which is contrary to the claim in ref. [45].

Since simulating QCD on a quantum computer remains a formidable task to date [65], we resort to a simple model, the Nambu-Jona-Lasinio (NJL) model [66, 67] in (1+1) dimensions, also known as the Gross-Neveu model [68], in order to demonstrate simulations of the LCDA on a quantum computer. The Lagrangian of the (1 + 1)D NJL model is given by

$$\mathcal{L} = \bar{\psi} (i\gamma^\mu \partial_\mu - m_q) \psi + g (\bar{\psi} \psi)^2, \quad (4)$$

where g is the strong coupling constant and m_q is the quark mass. The LCDA $\phi_h(x)$ of a meson h in the NJL model is defined by

$$\phi_h(x) = \frac{1}{f_h} \int dz e^{-i(x-1)n \cdot Pz} \times \langle \Omega | \bar{\psi}(zn) \gamma^+ \psi(0) | h(P) \rangle. \quad (5)$$

We note that the LCDA defined as in eq. (5) is independent of the frame of reference. For the sake of practical computation, we will evaluate the LCDA in the rest

frame of the meson, in which case we have

$$\phi_h(x) = \frac{1}{f_h} \int dz e^{-i(x-1)m_n z} \times \langle \Omega | e^{iHt} \bar{\psi}(0, -z) e^{-iHt} \gamma^+ \psi(0, 0) | h \rangle, \quad (6)$$

where we have written the quark field $\bar{\psi}(zn)$ as $\bar{\psi}(zn) = e^{iHz} \bar{\psi}(0, -z) e^{-iHz}$ with H the Hamiltonian of the NJL model, and we will set $t = z$ in eq. (6) to put the correlator on the light cone. Here m_h is the mass of the meson h .

To facilitate quantum simulations, we discretize the space into $N/2$ lattice sites and place the fermion field on the lattice following:

$$\psi(0, \mathbf{z}) = \begin{pmatrix} \psi_1(0, \mathbf{z}) \\ \psi_2(0, \mathbf{z}) \end{pmatrix} \equiv \begin{pmatrix} \varphi_{2n} \\ \varphi_{2n+1} \end{pmatrix}, \quad (7)$$

where $0 \leq n \leq \frac{N}{2} - 1$. Notice that, throughout this paper, the subscript n denotes the qubit index. Note that we have distributed the upper and lower component of the Dirac spinor to the even and odd lattice sites respectively. After performing the Jordan-Wigner transformation [69],

$$\varphi_n \equiv \Xi_n^3 \sigma_n^+, \quad (8)$$

the fields operator φ_n can be represented by quantum gates on a quantum circuit. Here we have introduced the raising and lowering operators $\sigma_n^\pm = \frac{1}{2}(\sigma_n^1 \pm i\sigma_n^2)$, and the string operator $\Xi_n^3 \equiv \prod_{n' < n} \sigma_{n'}^3$, with σ_n^j denoting the j -th component of the Pauli matrix on the qubit n . Throughout this study, we impose the periodic boundary condition. The LCDA then reads

$$\phi_h(x) = \frac{1}{f_h} \sum_z \frac{1}{4\pi} e^{-i(x-1)m_n z} \tilde{\phi}_h(z), \quad (9)$$

where

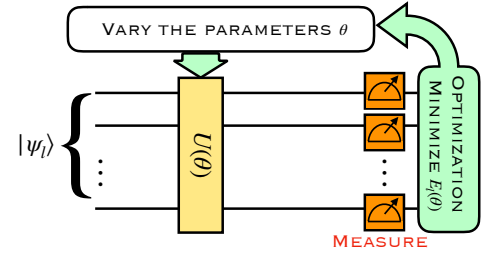
$$\tilde{\phi}_h(z) = \sum_{i,j=0}^1 \langle \Omega | e^{iHz} \varphi_{-2z+i}^\dagger e^{-iHz} \varphi_j | h \rangle. \quad (10)$$

III. QUANTUM ALGORITHM FOR LCDAS

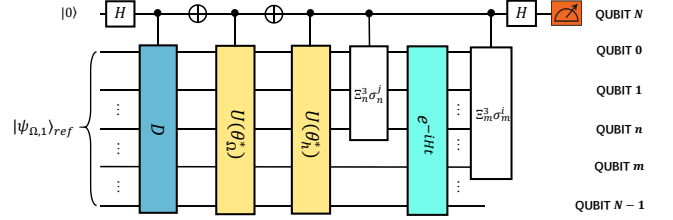
We implement the quantum algorithm proposed in Ref. [51] to simulate the real-time light-cone correlator. The quantum algorithm is described by the quantum circuit shown in Fig. 1, which consists of two parts: preparation of the hadronic state and evaluation of the correlator. Note that the vacuum state can be prepared as a particular case of a hadronic state.

A. Preparation of the hadronic state

The preparation of the hadronic state is achieved by the quantum-number-resolving variational quantum



(a) Quantum circuit for preparation of the hadronic state



(b) Quantum circuit for the correlator $\langle \Omega | \mathcal{O} | h \rangle$

FIG. 1. Quantum circuit for calculation of the LCDA. Diagram (a) gives the circuit for hadronic state preparation, while (b) is for evaluation of the correlator.

eigensolver (VQE), summarized as follows. To find the first k excited states $|h\rangle$ with quantum numbers l , we construct the trial states $|\psi_{li}(\theta)\rangle$, $i = 1, 2, \dots, k$, ($i = 1$ corresponds to the lowest-lying state) by

$$|\psi_{li}(\theta)\rangle = U(\theta) |\psi_{li}\rangle_{\text{ref}}, \quad (11)$$

where $|\psi_{li}\rangle_{\text{ref}}$ are some input reference states with the same quantum numbers l as the hadron states $|h\rangle$, and $U(\theta)$ a symmetry-preserving unitary operator with parameters θ . Since $U(\theta)$ preserves the quantum numbers, all of the trial states will have the same quantum numbers as $|h\rangle$. Then we can find out the hadron states among the trial states by minimizing the cost function

$$E_l(\theta) = \sum_{i=1}^k w_{li} \langle \psi_{li}(\theta) | H | \psi_{li}(\theta) \rangle. \quad (12)$$

Here we require $w_{l1} > w_{l2} > \dots > w_{lk}$. The i -th excited state $|h\rangle$ is then prepared as $|h\rangle = U(\theta^*) |\psi_{li}\rangle_{\text{ref}}$ with θ^* the optimized values of θ . In the following, we describe in detail how the input reference states are prepared, and how the operator $U(\theta)$ is constructed with the quantum alternating operator ansatz (QAOA).

1. Preparation of input reference states

We complete the quantum algorithm framework for preparing hadronic states with detailed constructions of

the input states. The input states have the same quantum numbers as the hadron and in general, they should be superposed states of the computational basis. We find that the input states are closely related to the so-called Dicke states, whose efficient preparation with explicit quantum circuits is available in Ref. [70]. To study generic hadronic states on a quantum computer, we outline the basic construction of the quantum circuit for the Dicke states.

In the NJL model, to prepare the lightest $|q\bar{q}\rangle$ state that has the same quantum numbers as the vacuum, the N -qubit zero-momentum input state of the QAOA can be chosen as:

$$\begin{aligned} |\psi_{\Omega,1}\rangle_{\text{ref}} &= |010101\dots 01\rangle, \\ |\psi_{\Omega,2}\rangle_{\text{ref}} &= \frac{1}{\sqrt{N/2}} (|1001\dots 01\rangle + |0110\dots 01\rangle \\ &\quad + \dots + |0101\dots 10\rangle), \end{aligned} \quad (13)$$

where $|x_1x_2\dots x_n\rangle$ with $x_1, x_2, \dots, x_n = 0, 1$ are the computational basis states for an n -qubit system [71], both $|\psi_{\Omega,1}\rangle_{\text{ref}}$ and $|\psi_{\Omega,2}\rangle_{\text{ref}}$ share the same quantum numbers with the $|q\bar{q}\rangle$ state. The state $|\psi_{\Omega,1}\rangle_{\text{ref}}$ is a product state that can be easily prepared from the state $|0000\dots 00\rangle$. The preparation of the superposed state $|\psi_{\Omega,2}\rangle_{\text{ref}}$ is more involved, which we will focus on. We first denote $|\bar{0}\rangle \equiv |01\rangle$ and $|\bar{1}\rangle \equiv |10\rangle$ to write $|\psi_{\Omega,2}\rangle$ as:

$$|\psi_{\Omega,2}\rangle_{\text{ref}} = \sqrt{\frac{1}{C_{N/2}^1}} (|\bar{1}\bar{0}\dots\bar{0}\rangle + |\bar{0}\bar{1}\dots\bar{0}\rangle + |\bar{0}\bar{0}\dots\bar{1}\rangle). \quad (14)$$

It can be seen that $|\psi_{\Omega,2}\rangle_{\text{ref}}$ is closely related to the Dicke state $|D_1^{N/2}\rangle$ [70], which can be prepared by a series of split-and-cyclic-shift (SCS $_{n,1}$) gates as:

$$|D_1^{N/2}\rangle = \prod_{n=2}^{N/2} \text{SCS}_{n,1} |0\rangle^{\otimes \frac{N}{2}-1} |1\rangle. \quad (15)$$

The SCS $_{n,1}$ gates can be written as elementary controlled NOT (CNOT) and controlled R_y gates,

$$\begin{aligned} \text{SCS}_{n,1} &= \left[\text{CNOT}(n-1, n) \right. \\ &\quad \times \text{CR}_y \left(n, n-1, 2\cos^{-1} \sqrt{\frac{1}{n}} \right) \\ &\quad \left. \times \text{CNOT}(n-1, n) \right], \end{aligned} \quad (16)$$

where $\text{CNOT}(i, j)$ is the controlled NOT gate, with the qubit i being the control qubit and the NOT gate acting on the qubit j . $\text{CR}_y(i, j, \theta)$ is the controlled R_y gate, where i is the control qubit, and $R_y(\theta)$ acts on the qubit j as a rotation about the y -axis by an angle θ . To prepare

$|\psi_{\Omega,2}\rangle_{\text{ref}}$, we first prepare the Dicke state $|D_1^{N/2}\rangle$. Then to the right of each qubit we attach a new qubit initialized as $|0\rangle$ and perform a controlled-NOT gate operation so that $|00\rangle \rightarrow |01\rangle$ and $|10\rangle \rightarrow |10\rangle$. In this way, $|\psi_{\Omega,2}\rangle_{\text{ref}}$ can be prepared from the Dicke state with an additional layer of two-qubit gates. The quantum circuit to prepare $|\psi_{\Omega,2}\rangle_{\text{ref}}$ from the Dicke state $|D_1^{N/2}\rangle$ is shown in Fig. 2.

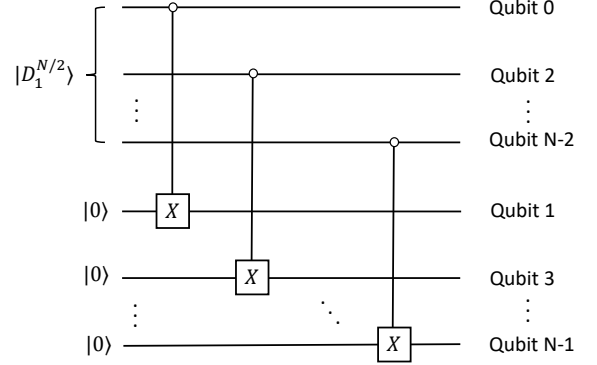


FIG. 2. Quantum circuit for preparing $|\psi_{\Omega,2}\rangle_{\text{ref}}$ from the Dicke state $|D_1^{N/2}\rangle$. The input state for the even qubits is the Dicke state and the input state for the odd qubits is the state $|0\rangle^{\otimes N/2}$.

As another example, the input state of $|qq\rangle$ can be prepared in the following way. Since $|qq\rangle$ is a superposition of configurations of two fermions in the odd sites while the even sites are empty, the input state is then a Dicke state $|D_2^{N/2}\rangle$ on the odd sites with all even sites at the state $|1\rangle$. Input states for other hadrons can be constructed in a similar fashion.

2. Constructing $U(\theta)$ with QAOA

The operator $U(\theta)$ can be constructed by the quantum alternating operator ansatz (QAOA). The Hamiltonian is split as $H = H_1 + H_2 + \dots + H_M$, where $M \geq 2$, with every H_i inheriting the symmetries of H and $[H_i, H_{i+1}] \neq 0$. Then $U(\theta)$ is given by

$$U(\theta) \equiv \prod_{i=1}^p \prod_{j=1}^M \exp(i\theta_{ij} H_j). \quad (17)$$

Because every H_i inherits the symmetries of H , the time evolution $\exp(i\theta_{ij} H_j)$ preserves the quantum numbers of the input reference state. The operator $\exp(i\theta_{ij} H_j)$ can be regarded as a rotation in the high-dimensional Hilbert space about the axis H_i . The larger the M , the more choices of rotational axes we have. Furthermore, since $[H_i, H_{i+1}]$ does not vanish, successive rotations about H_i and H_{i+1} are equivalent to a rotation about a new axis. Therefore, the larger the values of p and M , the better

are the true hadronic states approximated by the trial states after the optimization. It should be noted that the required size of p depends on the value of the bare coupling g . If g is small, say $g \sim 0.1$, p can be chosen to be N ; while if $g \sim 0.5$, p can be chosen to be $N/2$. Optimization is achieved by minimizing the cost function.

In our case of the (1+1)D 1-flavor NJL model with staggered fermions, after the Jordan-Wigner transformation, the original Hamiltonian H is split as $H = H_1 + H_2 + H_3 + H_4$, with

$$\begin{aligned}
 H_1 &= \sum_{n=\text{even}}^{\frac{N}{2}-1} \frac{1}{4} (\sigma_n^1 \sigma_{n+1}^2 - \sigma_n^2 \sigma_{n+1}^1), \\
 H_2 &= \sum_{n=\text{even}}^{\frac{N}{2}-1} \frac{g}{2} \sigma_n^3 \sigma_{n+1}^3, \\
 H_3 &= H_1 (n = \text{even} \rightarrow n = \text{odd}) \\
 &\quad + \frac{1}{4} \Xi_{N-1}^3 (\sigma_{N-1}^2 \sigma_0^1 - \sigma_{N-1}^1 \sigma_0^2), \\
 H_4 &= \sum_{n=0}^{\frac{N}{2}-1} \frac{m_q}{2} (-1)^n (I - \sigma_n^3) - \frac{g}{2} (I - \sigma_n^3). \quad (18)
 \end{aligned}$$

We will consider the lowest-lying scalar meson state, i.e. the lightest hadron state $|h\rangle$ with the same quantum numbers as the vacuum.¹ The input reference states are as in eq. (13).

B. Evaluation of the correlator

For evaluation of the correlator, as depicted in Fig. 1(b), with the help of an ancillary qubit we measure the correlation function

$$S_{mn}(t) = \langle \Omega | e^{iHt} \Xi_m^3 \sigma_m^i e^{-iHt} \Xi_n^3 \sigma_n^j | h \rangle, \quad (19)$$

of which $\tilde{\phi}_h(z)$ in eq. (10) can be written as a sum (see Ref. [51] for details). In Fig. 1(b), the input state of the quantum circuit is taken as $|\psi_{\Omega,1}\rangle_{\text{ref}} = |0101, \dots, 01\rangle$. The quantum gate D is implemented for preparation of the Dicke state for the reference hadron state: $D |\psi_{\Omega,1}\rangle_{\text{ref}} = |\psi_h\rangle_{\text{ref}}$. The unitary gate $U(\theta_\Omega^*)$ and $U(\theta_h^*)$ can help us prepare the vacuum and the hadronic state: $U(\theta_\Omega^*) |\psi_{\Omega,1}\rangle_{\text{ref}} = |\Omega\rangle$, $U(\theta_h^*) |\psi_h\rangle_{\text{ref}} = |h\rangle$. Specifically, if we want to prepare the k -th excited hadronic state with the same quantum numbers l as the vacuum state, we have $|\psi_h\rangle_{\text{ref}} = |\psi_{\Omega,k}\rangle_{\text{ref}}$ and $\theta_h^* = \theta_\Omega^*$. Acting the controlled gates D , $U(\theta_\Omega^*)$, and $U(\theta_h^*)$ on the circuit will facilitate evaluation of the dynamical correlation function $\langle \Omega | \mathcal{O} | h \rangle$, in which the bra state is different from the ket state. In short, when we act all the gates before

the controlled $\Xi_n^3 \sigma_n^j$ gate in the circuit, the state looks like $\frac{1}{\sqrt{2}}(|0\rangle |\Omega\rangle + |1\rangle |h\rangle)$. After acting the controlled Pauli operators and the time evolution on the quantum circuit, we trace out the system and obtain the density matrix ρ_A of the ancillary qubit. The $(\rho_A)_{12}$ will have the form $\langle \Omega | \mathcal{O} | h \rangle$ since the states $|0\rangle$ and $|1\rangle$ of the ancillary qubit are entangled with $|\Omega\rangle$ and $|h\rangle$ respectively.

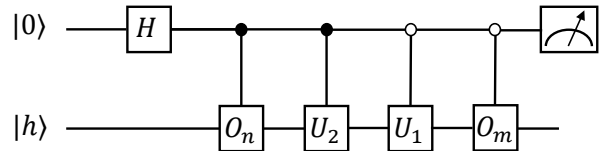


FIG. 3. Quantum circuit for the Hadamard test. The input state for the ancillary qubit is $|0\rangle$ and the input state for the system is the hadronic state $|h\rangle$.

It should be noted that, in the case of QCD, inclusion of the Wilson line will complicate the quantum circuit for the evaluation of the light-cone correlator. With the Wilson line, the light-cone correlator can still be expressed as a sum of $S_{mn}(t) = \langle h | U_1(t) O_m U_2(t) O_n | h \rangle$, where U_1 and U_2 are unitary operators, and O_m and O_n are Hermitian operators. However, unlike the case without the Wilson line, now we have $U_1(t) U_2(t) \neq 1$. When O_m and O_n are the Pauli operators, which are unitary, $S_{mn}(t)$ can be viewed as an overlap between the states $U_1(t) O_m U_2(t) O_n | h \rangle$ and $| h \rangle$, which can be evaluated with the standard Hadamard test, the quantum circuit of which is shown in Fig. 3.

IV. RESULTS

The classical simulation of the quantum algorithm is performed on a desktop workstation with 16 cores, using opensource packages QuSpin [72] and projectQ [73]. We perform the simulation of the LCDA for the lowest-lying scalar meson in the (1+1)D 1-flavor NJL model with $N = 14$ qubits and different values of the bare coupling constant g and hadron mass m_h . In practice, we first choose the values of the two free dimensionless parameters $m_q a$ and g , then from which we can determine the hadron state $|h\rangle$, its mass m_h in units of a^{-1} , as well as its LCDA. The values of $m_q a$ and g are chosen in such a way that the condition $\frac{2\pi}{Na} < m_h < \frac{\pi}{a}$ is satisfied, so that the lattice size is bigger than the hadron size and the lattice spacing is smaller than the hadron size. We choose the phase of the hadronic state $|h\rangle$ such that $\phi_h(x)$ is a real function.

We show in Figs. 4 and 5 the results for the real part and imaginary part of the LCDA in position space $\tilde{\phi}_h(z)$, respectively, with fixed value of $m_h = 1.5a^{-1}$ and different values of g . We also show as dotted lines the inverse Fourier transform of the asymptotic form of $\phi_h(x)$

¹ Note that in reality the lightest hadron in QCD has different parity from the vacuum.

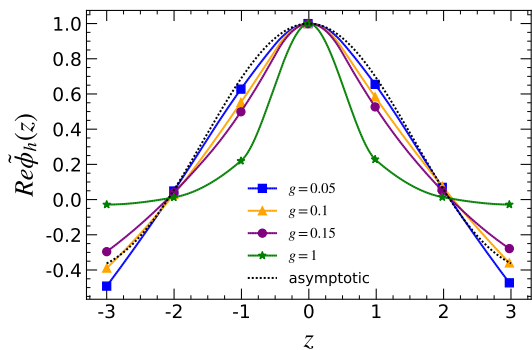


FIG. 4. Real part of $\tilde{\phi}_h(z)$ in the (1+1)D 1-flavor NJL model with $N = 14$, $m_h = 1.5a^{-1}$.

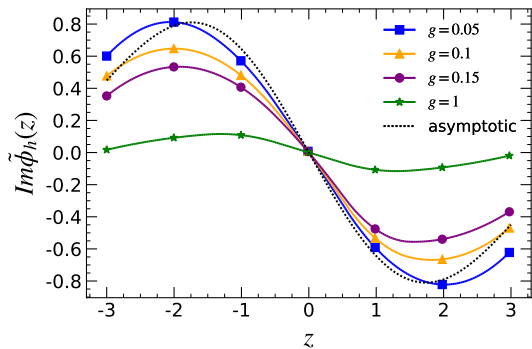


FIG. 5. Imaginary part of $\tilde{\phi}_h(z)$ in the (1+1)D 1-flavor NJL model with $N = 14$, $m_h = 1.5a^{-1}$.

in QCD, namely $\phi_{\text{asympt}}(x) = 6x(1-x)$ [5]. One notices that, as expected, the result from the quantum algorithm converges to the asymptotic LCDA as $g \rightarrow 0$, which mimics the asymptotic behavior of LCDAs in QCD.

Now we can evaluate the LCDA $\phi_h(x)$ by taking the Fourier transform of $\tilde{\phi}_h(z)$ as described in eq. (9). The final results are shown in Fig. 6, where the curves represent the results from exact diagonalization (ED), which are obtained from numerically diagonalizing the discretized NJL Hamiltonian, and the discrete open markers denote the results from quantum computing (QC) using classical hardware simulation. The excellent agreement between the results from the quantum algorithm and those from exact diagonalization justifies the designed quantum algorithm. Similar to Figs. 4 and 5, we also show the asymptotic form of $\phi_h(x)$ in QCD for comparison. As expected, the peak of the LCDA gets narrower and converges to the asymptotic LCDA as $g \rightarrow 0$. Notice that there is non-vanishing but suppressed contributions in the nonphysical region ($x > 1$ or $x < 0$). Such unphysical oscillations are caused by finite volume effects in the naively truncated Fourier transform, and are also commonly seen in lattice QCD calculations [29]. We also check the dependence of the LCDA on the hadron mass m_h in Fig. 7. For this purpose,

we take $m_h = 1.3a^{-1}, 1.5a^{-1}, 1.7a^{-1}$, and fix the bare coupling constant $g = 0.1$, with $N = 14$. One can see that the peak of $\phi_h(x)$ gets narrower when the hadron mass increases. This is the expected behavior when the valence quark and antiquark become nonrelativistic, in which case the quark masses dominate the momenta of the quark and antiquark, while the relative momentum between the two becomes small. The behavior also agrees with the results from lattice QCD [29]. We leave the extrapolation to the continuum limit as a follow-up work in the future.

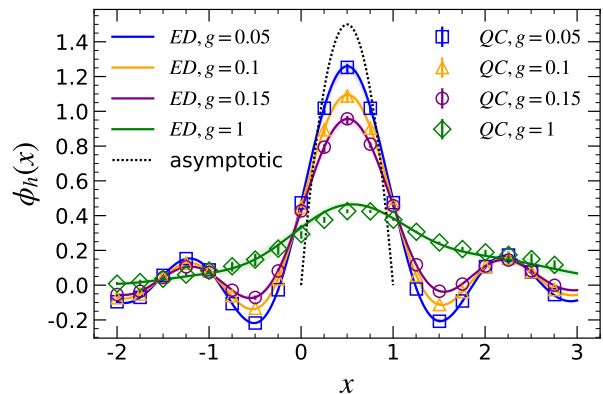


FIG. 6. LCDA in the (1+1)D 1-flavor NJL model with $N = 14$, $m_h = 1.5a^{-1}$.

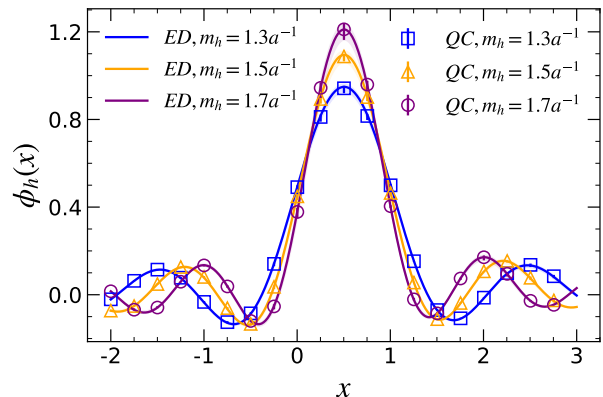


FIG. 7. Dependence of the LCDA on the hadron mass m_h with fixed bare coupling $g = 0.1$ in the (1+1)D 1-flavor NJL model.

V. SUMMARY

In this study, we presented the first direct simulation of the light-cone distribution amplitude (LCDA) with a quantum algorithm on classical hardware. Using a quantum algorithm we proposed recently for the evaluation of the parton distribution functions, here we performed

the simulation for the LCDA in the (1+1)-dimensional Nambu-Jona-Lasinio (NJL) model on classical hardware. With 14 qubits, our results from the quantum algorithm agree with those from exact diagonalization of the discretized NJL model. Our results of the LCDA showed the expected dependence on the coupling constant and the hadron mass.

The result presented in this study manifests the feasibility of using quantum computing to solve intrinsic difficulties in realizing real-time dynamics with classical computing facilities. Meanwhile, it demonstrates that the recently proposed quantum computing framework for preparing hadronic states and measuring dynamical correlation functions is generally applicable. The extension of the algorithm to other applications in high energy particle and nuclear physics can be expected.

ACKNOWLEDGMENTS

This work is supported by the National Natural Science Foundation of China under Grant No. 12022512, No. 12035007 (H.X.), Grant No. 12175016 (X.L.), Grant No.12005065 (D.B.), Grant No. 12074180 (S.L.), and by the Guangdong Major Project of Basic and Applied Basic Research No. 2020B0301030008, the Key-Area Research and Development Program of Guangdong Province (Grant No. 2019B030330001), the Guangdong Basic and Applied Basic Research Fund No.2021A1515010317 (D.B.), the Key Project of Science and Technology of Guangzhou (Grant No. 2019050001), the National Special Support Program for High-level Talents (X.L.).

-
- [1] H. Abramowicz *et al.*, Eur. Phys. J. C **75**, no.12, 580 (2015)
- [2] R. Abdul Khalek, A. Accardi, J. Adam, D. Adamiak, W. Akers, M. Albaladejo, A. Al-bataineh, M. G. Alexeev, F. Ameli and P. Antonioli, *et al.* Nucl. Phys. A **1026**, 122447 (2022)
- [3] Cao, X. *et al.*, Nucl. Tech., **43**, 020001 (2020).
- [4] D. P. Anderle, V. Bertone, X. Cao, L. Chang, N. Chang, G. Chen, X. Chen, Z. Chen, Z. Cui and L. Dai *et al.*, Front. Phys. **16**, 64701 (2021).
- [5] G. P. Lepage and S. J. Brodsky, Phys. Rev. D **22**, 2157 (1980).
- [6] A. V. Efremov and A. V. Radyushkin, Phys. Lett. B **94**, 245 (1980).
- [7] V. L. Chernyak and A. R. Zhitnitsky, Phys. Rep. **112**, 173 (1984).
- [8] V. L. Chernyak and A. R. Zhitnitsky, Nucl. Phys. B **201**, 492 (1982), [Erratum: Nucl.Phys.B 214, 547 (1983)].
- [9] V. L. Chernyak and I. R. Zhitnitsky, Nucl. Phys. B **246**, 52 (1984).
- [10] I. D. King and C. T. Sachrajda, Nucl. Phys. B **279**, 785 (1987).
- [11] V. L. Chernyak, A. A. Ogloblin, and I. R. Zhitnitsky, Yad. Fiz. **48**, 1410 (1988).
- [12] V. L. Chernyak, A. A. Ogloblin, and I. R. Zhitnitsky, Yad. Fiz. **48**, 1398 (1988).
- [13] A. V. Radyushkin, Nucl. Phys. A **532**, 141 (1991).
- [14] E. Ruiz Arriola and W. Broniowski, Phys. Rev. D **74**, 034008 (2006), arXiv:hep-ph/0605318.
- [15] E. Ruiz Arriola and W. Broniowski, Phys. Rev. D **66**, 094016 (2002), arXiv:hep-ph/0207266.
- [16] L. Chang *et al.*, Phys. Rev. Lett. **110**, 132001 (2013), arXiv:1301.0324.
- [17] S. S. Agaev, V. M. Braun, N. Offen, and F. A. Porkert, Phys. Rev. D **86**, 077504 (2012), arXiv:1206.3968.
- [18] S. J. Brodsky and G. F. de Teramond, Phys. Rev. Lett. **96**, 201601 (2006)
- [19] J. P. Vary, H. Honkanen, J. Li, P. Maris, S. J. Brodsky, A. Harindranath, G. F. de Teramond, P. Sternberg, E. G. Ng and C. Yang, Phys. Rev. C **81**, 035205 (2010)
- [20] S. J. Brodsky, G. F. de Teramond, H. G. Dosch and J. Erlich, Phys. Rep. **584**, 1-105 (2015)
- [21] S. Xu *et al.* [BLFQ], Phys. Rev. D **104**, no.9, 094036 (2021)
- [22] J. P. Ma and Z. G. Si, Phys. Lett. B **647**, 419 (2007), arXiv:hep-ph/0608221.
- [23] Y. Jia and D. Yang, Nucl. Phys. B **814**, 217 (2009), arXiv:0812.1965.
- [24] M. Gockeler *et al.*, Phys. Rev. Lett. **101**, 112002 (2008), arXiv:0804.1877.
- [25] V. M. Braun *et al.*, Phys. Rev. D **79**, 034504 (2009), arXiv:0811.2712.
- [26] V. M. Braun *et al.*, Phys. Rev. D **89**, 094511 (2014), arXiv:1403.4189.
- [27] G. S. Bali *et al.*, J. High Energ. Phys. **02**, 070 (2016), arXiv:1512.02050.
- [28] G. S. Bali *et al.*, J. High Energ. Phys. **08**, 065 (2019), arXiv:1903.08038.
- [29] R. Zhang, C. Honkala, H.-W. Lin, and J.-W. Chen, Phys. Rev. D **102**, 094519 (2020), arXiv:2005.13955.
- [30] J.-H. Zhang, J.-W. Chen, X. Ji, L. Jin, and H.-W. Lin, Phys. Rev. D **95**, 094514 (2017), arXiv:1702.00008.
- [31] J.-H. Zhang *et al.*, Nucl. Phys. B **939**, 429 (2019), arXiv:1712.10025.
- [32] J. Hua *et al.*, Phys. Rev. Lett. **127**, 062002 (2021), arXiv:2011.09788.
- [33] J. Hua *et al.*, arXiv:2201.09173.
- [34] A. Alexandru, G. Basar, P. F. Bedaque, S. Vartak, and N. C. Warrington, Phys. Rev. Lett. **117**, 081602 (2016), arXiv:1605.08040.
- [35] F. Arute *et al.*, Nature **574**, 505 (2019), arXiv:1910.11333.
- [36] M. R. Dietrich *et al.*, Opportunities for Nuclear Physics and Quantum Information Science, arXiv:1903.05453.
- [37] D.-B. Zhang, H. Xing, H. Yan, E. Wang, and S.-L. Zhu, Chin. Phys. B **30**, 020306 (2021), arXiv:2011.01431.
- [38] C. W. Bauer *et al.*, arXiv:2204.03381.
- [39] S. P. Jordan, K. S. M. Lee, and J. Preskill, Science **336**, 1130 (2012), arXiv:1111.3633.
- [40] S. P. Jordan, K. S. M. Lee, and J. Preskill, Quant. Inf. Comput. **14**, 1014 (2014), arXiv:1112.4833.
- [41] S. P. Jordan, K. S. M. Lee, and J. Preskill,

- arXiv:1404.7115.
- [42] N. Klco and M. J. Savage, Phys. Rev. A **99**, 052335 (2019), arXiv:1808.10378.
- [43] E. F. Dumitrescu *et al.*, Phys. Rev. Lett. **120**, 210501 (2018), arXiv:1801.03897.
- [44] H.-H. Lu *et al.*, Phys. Rev. A **100**, 012320 (2019), arXiv:1810.03959.
- [45] H. Lamm, S. Lawrence, and Y. Yamauchi, Phys. Rev. Res. **2**, 013272 (2020), arXiv:1908.10439.
- [46] N. Mueller, A. Tarasov, and R. Venugopalan, Phys. Rev. D **102**, 016007 (2020), arXiv:1908.07051.
- [47] A. Roggero, A. C. Y. Li, J. Carlson, R. Gupta, and G. N. Perdue, Phys. Rev. D **101**, 074038 (2020), arXiv:1911.06368.
- [48] M. G. Echevarria, I. L. Egusquiza, E. Rico, and G. Schnell, arXiv:2011.01275.
- [49] C. W. Bauer, M. Freytsis, and B. Nachman, arXiv:2102.05044.
- [50] Y. Y. Atas *et al.*, Nature Commun. **12**, 6499 (2021), arXiv:2102.08920.
- [51] T. Li *et al.*, Phys. Rev. D **105**, L111502 (2022), arXiv:2106.03865.
- [52] M. Kreshchuk, S. Jia, W. M. Kirby, G. Goldstein, J. P. Vary and P. J. Love, Entropy **23**, no.5, 597 (2021)
- [53] D. Gallimore and J. Liao, arXiv:2202.03333.
- [54] E. A. Martinez *et al.*, Nature **534**, 516 (2016), arXiv:1605.04570.
- [55] Z. Hu, R. Xia, and S. Kais, Sci. Rep. **10**, 3301 (2020), arXiv:1904.00910.
- [56] C. W. Bauer, W. A. de Jong, B. Nachman, and D. Provasoli, Phys. Rev. Lett. **126**, 062001 (2021), arXiv:1904.03196.
- [57] W. A. De Jong *et al.*, Phys. Rev. D **104**, 051501 (2021), arXiv:2010.03571.
- [58] Z.-Y. Zhou *et al.*, arXiv:2107.13563.
- [59] W. A. de Jong *et al.*, arXiv:2106.08394.
- [60] S. Williams, S. Malik, M. Spannowsky, and K. Bepari, arXiv:2109.13975.
- [61] Y. Y. Atas *et al.*, arXiv:2207.03473.
- [62] X. Yao, arXiv:2205.07902.
- [63] A. M. Czajka, Z.-B. Kang, H. Ma, and F. Zhao, arXiv:2112.03944.
- [64] X.-D. Xie *et al.*, arXiv:2205.12767.
- [65] M. C. Bañuls *et al.*, Eur. Phys. J. D **74**, 165 (2020), arXiv:1911.00003.
- [66] Y. Nambu and G. Jona-Lasinio, Phys. Rev. **122**, 345 (1961).
- [67] Y. Nambu and G. Jona-Lasinio, Phys. Rev. **124**, 246 (1961).
- [68] D. J. Gross and A. Neveu, Phys. Rev. D **10**, 3235 (1974).
- [69] S. Backens, A. Shnirman, and Y. Makhlin, Sci. Rep. **9** (2019).
- [70] A. Bärttschi and S. Eidenbenz, Deterministic preparation of dicke states, in L.A. Gasienice, J. Jansson, and C. Levcopoulos, eds., *Fundamentals of Computation Theory* (Springer, Cham,2019), pp. 126–139.
- [71] M. A. Nielsen, and I.L. Chuang, *Quantum Computation and Quantum Information* (Cambridge University Press, Cambridge, 2010).
- [72] P. Weinberg and M. Bukov, SciPost Phys. **2**, 003 (2017).
- [73] D. S. Steiger, T. Häner, and M. Troyer, Quantum **2**, 49 (2018).